



HAL
open science

Adaptive Feedforward Super-Twisting Sliding Mode Control of Parallel Kinematic Manipulators With Real-Time Experiments

Hussein Saied, Ahmed Chemori, Mohamed Bouri, Maher El Rafei, Clovis Francis

► **To cite this version:**

Hussein Saied, Ahmed Chemori, Mohamed Bouri, Maher El Rafei, Clovis Francis. Adaptive Feedforward Super-Twisting Sliding Mode Control of Parallel Kinematic Manipulators With Real-Time Experiments. IROS 2024 - IEEE/RSJ International Conference on Intelligent Robots and Systems, Oct 2024, Abu Dhabi, United Arab Emirates. lirmm-04661496

HAL Id: lirmm-04661496

<https://hal-lirmm.ccsd.cnrs.fr/lirmm-04661496>

Submitted on 24 Jul 2024

HAL is a multi-disciplinary open access archive for the deposit and dissemination of scientific research documents, whether they are published or not. The documents may come from teaching and research institutions in France or abroad, or from public or private research centers.

L'archive ouverte pluridisciplinaire **HAL**, est destinée au dépôt et à la diffusion de documents scientifiques de niveau recherche, publiés ou non, émanant des établissements d'enseignement et de recherche français ou étrangers, des laboratoires publics ou privés.

Adaptive Feedforward Super-Twisting Sliding Mode Control of Parallel Kinematic Manipulators With Real-Time Experiments

Hussein Saied^{1,3}, Ahmed Chemori¹, Mohamed Bouri², Maher El Rafei³ and Clovis Francis⁴

Abstract— In this paper, we propose a novel adaptive feedforward super-twisting sliding mode control algorithm to resolve the tracking control problem of parallel manipulators. The proposed control scheme includes three main terms, (i) the standard super-twisting algorithm, (ii) an adaptive feedforward dynamic model, and (iii) a feedback term to ensure stability. The proposed controller provides robustness towards uncertainties and disturbances, less sensitive to measurement noise, and allows dynamic parameters adaptation of the manipulator while executing a certain task. Real-time experiments are conducted on a 3-DOF non-redundant Delta parallel robot, including two main scenarios, (i) nominal case, and (ii) robustness towards operating acceleration changes. The relevance of the proposed controller is verified experimentally in both scenarios and compared with two other controllers from the literature, including the standard and the feedforward super-twisting sliding mode control algorithms.

I. INTRODUCTION

The interest in Parallel Kinematic Manipulators (PKMs) has increased in the last decades due to their advantages compared to their serial counterparts. PKMs offer high stiffness and, subsequently, high accuracy, operations at very high accelerations, and a high payload-to-weight ratio. However, PKMs suffer from a limited workspace, abundant singularities inside and on the borders of the workspace, and complex kinematic and dynamic modeling. Nowadays, PKMs are contributing to many sectors and fields such as industry (food packaging [1], machining tasks [2]), medicine (precise surgical interventions [3]), recycling (robotized waste sorting [4]), and aeronautics (flight simulators [5]). Consequently, control of PKMs is a key factor in improving their performance and thereby improving the efficiency of the conducted tests in these sectors.

Control of PKMs can be considered a challenging task due to several factors such as: i) high effect of nonlinear dynamics of PKMs especially when operating at high accelerations, ii) coupled dynamics that need careful control synchronization among actuators, iii) unstructured uncertainties emerging from geometric errors, modeling simplifications, disturbances, etc., and iv) structural uncertainties that appear in the form of inaccurate knowledge about the dynamic parameters (payload, external contact forces, etc.).

A vast range of control schemes have been proposed in the literature to solve the control problem of PKMs. One can classify the existing controllers into two main classes:

non-model-based and model-based approaches as detailed in the sequel.

Non-model-based controllers are closed-loop algorithms that do not need a priori knowledge about the dynamic model of the PKM. This type of controllers is designed using a feedback of the manipulator states (e.g. positions and velocities). The Proportional-Integral-Derivative (PID) controller is the most famous algorithm in industrial PKM applications due to its simplicity and easy implementation [6]. However, classical PID controller lacks robustness towards nonlinearities induced by operating conditions (e.g. acceleration). Thus, nonlinear PD control proposed in [7] has shown better performances thanks to its disturbance rejection ability and robustness towards uncertainties. The Robust Integral of the Sign of the Error (RISE) has been applied to Delta PKM in [8], and compared to an extended version of RISE with nonlinear feedback gains. The proposed extended RISE control has shown better performances than the classical one thanks to robustness towards changes in operating conditions. Besides, in [9], a continuous modified twisting algorithm is designed for the position control of a Stewart platform. The relevance of the proposed controller has been proved through numerical simulations showing an accurate positioning despite the presence of matched disturbances.

Model-based controllers take into account the dynamic model of the PKM within the closed-loop scheme to compensate for its nonlinearity. PKM nonlinearities may considerably increase when operating at high accelerations. Model-based controllers can be classified into non-adaptive and adaptive schemes.

Non-adaptive model-based controllers are designed without adaptation of dynamic parameters. A PD control with gravity compensation term compensates for the effects of gravitational forces that may deteriorate the performance of a PKM [10]. Unlike PD control with gravity compensation, Augmented PD (APD) control compensates the effects of further dynamic parameters such as inertia and mass matrix, centrifugal and Coriolis forces, and the gravity [11]. Computed Torque (CT) control is based on a nonlinear compensation strategy that leads up to a linear closed-loop dynamic equation of the error [12]. This control relies on the feedback measurements and estimations. Thus, it needs a good knowledge of the parameters and may be computationally heavy. PD control with computed feedforward uses the full inverse dynamic model of a PKM within an offline computation mode based on the desired trajectory [13]. Good tracking performances of this controller have been validated for high-speed pick-and-place motions thanks to its robustness towards measurement noise and compensation for nonlinearities. Other non-adaptive model-based controllers may include model predictive control [14].

Adaptive dynamic controllers consider the dynamic model of PKMs providing an estimation of the uncertain, time-varying, and unknown parameters. Adaptive feedforward

*This work was not supported by any organization.

¹Hussein Saied and Ahmed Chemori are with LIRMM, University of Montpellier, CNRS, Montpellier, France, hussein.a.saied@gmail.com, Ahmed.Chemori@lirmm.fr

²Mohamed Bouri is with EPFL, Station 9, Lausanne CH-1015, Switzerland mohamed.bouri@epfl.ch

³Hussein Saied and Maher El Rafei are with CRSI, Faculty of Engineering, Lebanese University, Beirut, Lebanon maher.elrafei@ul.edu.lb

⁴Clovis Francis is with Arts et Métiers ParisTech, Campus de Châlons-en-Champagne, France clovis.francis@ensam.eu

controllers are designed based on two main terms: a feedback controller and an adaptive feedforward term. One can mention PD with adaptive feedforward control [15], dual-space adaptive feedforward control [16], RISE-based adaptive feedforward control [17], and adaptive terminal sliding mode control [18]. The experimental results ensure the boundedness and convergence of the estimated parameters to the real values using an adequate adaptation law. The proposed adaptive control laws has better tracking performances than conventional controllers and more robustness towards parameters variation.

SMC approach is a robust control strategy able to guarantee the convergence of the state variables on the sliding surface to the origin in the presence of disturbances and uncertainties. For the uncertain nature of parallel manipulators, SMC-based algorithms can be potential candidates to solve the problem of motion control. The second-order ST-SMC algorithm results in an exact finite-time convergence of the sliding variable as well as its derivative, a high accurate asymptotic convergence of the variable states, and a continuous control signal [19]. In [20], a feedforward ST-SMC algorithm has been tested experimentally on a PKM prototype verifying its relevance at different dynamic operating conditions. An adaptive dynamic ST-SMC has been proposed in [21] and applied to the controller design for hydraulic actuators of a 6-DOF PKM, Stewart platform. The internal dynamics of a hydraulic actuator has been taken into account, while the main dynamics of Stewart PKM are ignored such as: mass of the parts, inertia effects, payload variation, acceleration changes, gravitational effects, etc. The simulation results have been used to evaluate the stability and performance of the proposed approach, but the experimental validation is missing. **In [22] an adaptive-gain SMC methodology has been proposed, which operates without the need for predefined bounded uncertainty. An illustrative example has been provided to demonstrate the primary characteristics of this approach. Subsequently, the proposed design has been applied to a general class of Euler-Lagrange systems, such as PKMs, to validate its applicability.**

In this paper, a model-based adaptive dynamic Super-Twisting Sliding Model Control (ST-SMC) is proposed to solve the trajectory tracking problem of PKMs. It inherits the advantages of the ST-SMC algorithm such as robustness towards disturbances and uncertainties, providing a continuous control signal, and a finite-time convergence of the sliding variable and its derivative. It relies on an adaptive feedforward dynamic term that can compensate for nonlinearities of PKMs, cope with parameters' variation, being less sensitive to measurement noise, and being more computationally efficient. To the best knowledge of the authors, adaptive ST-SMC algorithm has never been experimentally tested on parallel manipulators. We summarize the contributions of this paper as follows: i) we extend the standard ST-SMC algorithm to an adaptive dynamic ST-SMC to solve the control problem of PKMs, ii) we validate the proposed control solution through extensive real-time experimental tests.

The rest of the paper is organized as follows. Section II introduces the conventional ST-SMC of PKMs. Section III details the proposed adaptive dynamic ST-SMC for PKMs. Section IV provides the model of our PKM prototype. In section V, experimental results are presented and discussed. Section VI concludes the paper and gives some future work.

II. CONVENTIONAL SUPER-TWISTING SMC OF PKMS

A. Dynamic model of PKMs

The standard inverse dynamic model of PKMs delivers the actuated joint forces given the positions, velocities, and accelerations of the end-effector. The joint space formulation of the inverse dynamics can be expressed as follows [23]:

$$\Gamma(t) = M(q)\ddot{q} + C(q, \dot{q})\dot{q} + G(q) + \zeta(t) \quad (1)$$

where $M(q) \in \mathbb{R}^{n \times n}$ denotes the inertia matrix of the robot, $C(q, \dot{q}) \in \mathbb{R}^{n \times n}$ is the Coriolis and centrifugal forces matrix, $G(q) \in \mathbb{R}^n$ is the gravitational forces vector, $\zeta \in \mathbb{R}^n$ represents the vector of external disturbances, uncertainties, and unmodeled dynamics, and $\Gamma(t) \in \mathbb{R}^n$ represents the actuation joint torques.

According to [23], the dynamic equation of PKMs can be formulated as affine in the parameters. Thus, the new formulation of the dynamic model of PKMs can be expressed as follows:

$$Y(q, \dot{q}, \ddot{q})\Theta = M(q)\ddot{q} + C(q, \dot{q})\dot{q} + G(q) \quad (2)$$

where $Y(., ., .) \in \mathbb{R}^{n \times p}$ is a regressor matrix of nonlinear functions of joints positions, velocities, and accelerations, with n being the number of actuated joints and p being the number of parameters. $\Theta \in \mathbb{R}^p$ denotes the vector of manipulator parameters, including the links' masses, moments of inertia, lengths, etc.

B. Classical Super-Twisting SMC

We introduce the state-space representation of a Single-Input-Single-Output (SISO) second order nonlinear uncertain system as follows:

$$\begin{cases} \dot{x}_1 = x_2 \\ \dot{x}_2 = u + f(x, t) \end{cases} \quad (3)$$

where $x = [x_1, x_2]^T$ is the system states vector, u is the control input, and $f(., .)$ is a nonlinear function representing the unknown bounded uncertainties and perturbations, such that $|f(., .)| \leq L$ with L being a positive constant.

The idea of ST-SMC is to design a control signal that drives the state variables, in finite time, to zero in the presence of uncertainties and perturbations $f(x, t)$ [19]. Moreover, ST-SMC provides continuous control signal avoiding the problem of chattering and its inherent disadvantages on mechanical systems. A sliding surface is then defined as follows:

$$s = x_2 + cx_1 \quad (4)$$

where c is a positive constant. The Super-Twisting SMC algorithm is formulated as follows:

$$\begin{cases} u = -k_1|s|^{\frac{1}{2}}\text{sign}(s) + w \\ \dot{w} = -k_2\text{sign}(s) \end{cases} \quad (5)$$

where k_1, k_2 are positive feedback gains. Both terms of the ST-SMC algorithm are continuous, multiplication of Signum function by continuous one and integration of Signum function. The global asymptotic stability with finite-time states convergence of such controller is addressed in [24].

C. Super-Twisting SMC of PKMs

Consider now the trajectory tracking control problem of a PKM with joint space tracking error defined as follows:

$$e = q_d - q \quad (6)$$

where q_d, q are the desired and actual joint positions respectively. The sliding surface can then be defined as follows:

$$s = \dot{e} + \lambda e \quad (7)$$

with λ being a positive control gain. Let us now define an auxiliary shifted desired trajectory as follows:

$$\dot{r} = \dot{q}_d + \lambda e \quad (8)$$

By considering the dynamic model of the PKM in (1), the sliding surface dynamics can be derived as follows:

$$\dot{s} = \ddot{r} + F - M^{-1}(q)\Gamma \quad (9)$$

where $F = M^{-1}(q)(C(q, \dot{q})\dot{q} + G(q) + \zeta)$ being the function of gathered uncertainties. The ST-SMC control input is selected in a way that drives \dot{s} to zero as in [25] for the control of a serial robotic arm. Thus, assuming ζ is bounded, the conventional ST-SMC algorithm can be designed for PKMs as follows:

$$\begin{aligned} \Gamma &= M(q)(\ddot{r} + \Gamma_{ST-SMC}) \\ \Gamma_{ST-SMC} &= k_1 |s|^{\frac{1}{2}} \text{sign}(s) + k_2 \int_0^t \text{sign}(s) d\tau \end{aligned} \quad (10)$$

The standard form of ST-SMC, Γ_{ST-SMC} , eliminates as much as possible all the perturbations and uncertainties represented by F leading to a tracking error convergence.

In order to compensate for further nonlinearities, one can propose the ST-SMC-based computed torque formulation as in [26], [27] for serial robotic arms control. The ST-SMC-based computed torque algorithm is expressed as follows:

$$\Gamma = M(q)(\ddot{r} + \Gamma_{ST-SMC}) + C(q, \dot{q})\dot{q} + G(q) \quad (11)$$

In (11), the modeled nonlinear dynamics appear directly in the control loop, and can be compensated. The standard form of ST-SMC, Γ_{ST-SMC} , eliminates as much as possible all the unknown perturbations, uncertainties, and parameters present in ζ .

The disadvantages of ST-SMC-based computed torque control can be summarized as follows [28]: i) it needs an exact dynamic model, ii) it can be considered more sensitive to measurements noise since it relies on feedback signals to compute the dynamic parameters, iii) it can be affected by modeling errors due to its high model dependency, and iv) it has a heavy computational burden.

III. PROPOSED ADAPTIVE SUPER-TWISTING SMC FOR PKMS

In [20], a feedforward ST-SMC algorithm has been proposed as a control solution of PKMs, avoiding most of the aforementioned disadvantages of the conventional ST-SMC. The feedforward ST-SMC has been validated experimentally on two PKM prototypes. Its relevance has been shown through improved performances thanks to its main features of (i) less sensitivity towards measurements noise, (ii) robustness of super-twisting algorithm, and (iii) compensating for structural uncertainties.

However, the feedforward ST-SMC algorithm does not take into account the time-varying parameters. Moreover, the

non-modeled phenomena and unstructured uncertainties are treated with the ST-SMC algorithm without any estimation of their real-values. Consequently, proposing an adaptation law to handle those aspects may enhance the global dynamic performance of a PKM in terms of precision and robustness towards changes in the operating conditions.

The feedforward ST-SMC algorithm proposed in [20] is given as follows:

$$\begin{aligned} \Gamma_{FF-ST-SMC} &= M(q_d)\ddot{q}_d + C(q_d, \dot{q}_d)\dot{q}_d + G(q_d) \\ &+ K_1 s + \Gamma_{ST-SMC} \end{aligned} \quad (12)$$

with

$$\begin{aligned} \Gamma_{ST-SMC} &= K_2 |s|^{\frac{1}{2}} \text{sign}(s) + w \\ \dot{w} &= K_3 \text{sign}(s) \end{aligned} \quad (13)$$

where $q_d, \dot{q}_d, \ddot{q}_d$ denote the desired joint positions, velocities, and accelerations of the PKM respectively. K_1, K_2, K_3 represent positive diagonal matrices of the control feedback gains.

In order to endow the feedforward ST-SMC algorithm with a parameter adaptation feature, the dynamic model part of the controller in (12) is reformulated, like the dynamic equation introduced in (2), as follows:

$$\begin{aligned} \Gamma_{FF-ST-SMC} &= Y(q_d, \dot{q}_d, \ddot{q}_d)\Theta \\ &+ K_1 s + \Gamma_{ST-SMC} \end{aligned} \quad (14)$$

Then, the proposed adaptive controller is designed by replacing the steady-state parameter vector Θ in equation (14) by its estimation $\hat{\Theta}$ as follows:

$$\begin{aligned} \Gamma_{AFF-ST-SMC}(t) &= Y(q_d, \dot{q}_d, \ddot{q}_d)\hat{\Theta}(t) \\ &+ K_1 s(t) + \Gamma_{ST-SMC}(t) \end{aligned} \quad (15)$$

The adaptation law responsible of updating the estimated parameter vector $\hat{\Theta}$ is given as follows:

$$\dot{\hat{\Theta}}(t) = \Xi Y^T(q_d, \dot{q}_d, \ddot{q}_d) s(t) \quad (16)$$

where $\hat{\Theta} \in \mathbb{R}^p$ represents the time derivative of the estimated parameters vector, and $\Xi \in \mathbb{R}^{p \times p}$ is a positive diagonal matrix of the adaptation gains.

The proposed adaptation mechanism adjusts online the values of the dynamic parameters and feeds them to the control law in (15). This can cancel the inherent nonlinearities of PKMs, cope with unstructured uncertainties, and handle the issue of time-varying parameters. Two main advantages of the proposed adaptation mechanism can be highlighted as follows: (i) it's simple structure based on the regressor and position-velocity feedback, and (ii) the nonlinear regressor matrix relies on the desired trajectories instead of measured ones which can reduce the sensitivity to measurements noise. Consequently, the robustness of the control loop towards disturbances can thereby be enhanced.

IV. DELTA ROBOT: A 3-DOF NON-REDUNDANT PKM

A. Description of Delta PKM

The Delta robot is a 3-DOF non-redundant parallel manipulator. It has been developed at École Polytechnique Fédérale de Lausanne (EPFL), Switzerland, by professor Reymond Clavel [29]. The targeted application of this robot is fast pick-and-place operations that require high performance and precision. Fig. 1 illustrates a 3D schematic view of Delta parallel robot. The overall structure of this PKM is composed

as follows. A fixed base holds three actuators. Each actuator is connected to a rear arm through a revolute joint. Each rear arm is linked to a forearm, formed of two parallel rods, through a spherical joint. Thereafter, a traveling-plate is attached to the three forearms from other extremities, also through spherical joints, leading to a parallel mechanism. The resulting structure allows the traveling-plate to move along three axes: x , y , and z while preserving the parallelism of the traveling-plate with respect to the fixed base.

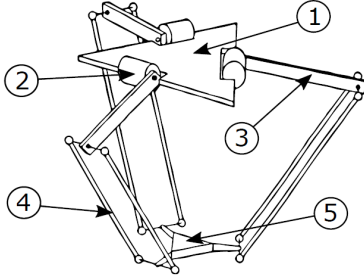


Fig. 1. A 3D schematic view of Delta parallel robot including ①: Fixed base, ②: Actuator, ③: Rear-arm, ④: Forearm, ⑤: Traveling-plate.

B. Kinematics of Delta PKM

The kinematic model formulates the relationship between the actuated joint angles and the Cartesian position of the traveling plate. Let us define the joint position vector as $q = [q_1, q_2, q_3]^T$ and the Cartesian position vector of the nacelle as $X = [x, y, z]^T$. One can find geometrical relations between X and q within the form of Inverse Kinematic (IK) and Forward Kinematic (FK) solutions expressed respectively as follows: $q = IK(X)$ and $X = FK(q)$. Differentiating the forward kinematic model with respect to time leads to establishing the relation between actuated joint velocities and Cartesian velocities of the traveling plate using the Jacobian matrix. This differential kinematic model is expressed as follows: $\dot{X} = J\dot{q}$ and $\dot{q} = J^{-1}\dot{X}$.

C. Dynamics of Delta PKM

The following assumptions, common for Delta-like PKMs modeling, can be considered for simplification purposes [30]:

Assumption 4.1: The inertia of the forearms can be neglected since the mass of one forearm is much smaller than the one of the rear arm (see Table I).

Assumption 4.2: The mass of each forearm is divided into two equal point-masses. The contribution of the first point-mass is added to the dynamics of the rear-arm, and the contribution of the second one is added to the dynamics of the traveling-plate (see illustration of Fig. 2).

The inverse dynamic model can be formulated using the virtual work principle which states that the contribution of all non-inertial forces is equal to that of all inertial forces [31]. One can consider the dynamics of Delta PKM at two levels: rear arms level and traveling-plate level.

On the one hand, at the level of the traveling plate, two forces are to be considered: gravitational and inertial. The gravitational force, acting on the traveling-plate, is expressed as follows:

$$G_{tp} = -M_{tp}G \quad (17)$$

where $M_{tp} = \text{diag}\{m_{tp}, m_{tp}, m_{tp}\}$ is the mass matrix of the traveling-plate with m_{tp} being the mass including the

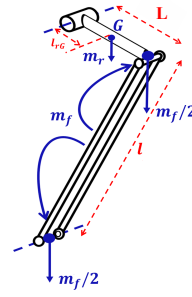


Fig. 2. Illustration of dynamic parameters of Delta parallel robot arm.

traveling-plate and the half masses of the forearms ($m_{tp} = m_p + 3\frac{m_f}{2}$), $G = [0, 0, g]^T$ is the gravitational vector with $g = 9.81 \text{ m/s}^2$ being the gravity acceleration. The inertial force, coming from the acceleration of the traveling-plate, is expressed as follows:

$$F_{tp} = M_{tp}\ddot{X} \quad (18)$$

On the other hand, the dynamics at the level of rear arms includes the torques generated by the actuators, the gravitational forces acting on the rear arms, and the inertial effects due to acceleration. Knowing that the torque is the cross product of the distance vector (i.e. the distance from the point of rotation to the point where force is applied) and the force vector. The torque contribution of the gravitational forces can be formulated as follows:

$$\Gamma_{G_{arm}} = -gM_r \text{Cos}(q) \quad (19)$$

where $M_r = \text{diag}\{m_{req}, m_{req}, m_{req}\}$ with $m_{req} = m_r l_r G + L\frac{m_f}{2}$ and m_r is the mass of the rear arm, $l_r G$ is the distance from the axis of rotation of the rear arm to its center of gravity, L is the length a rear arm, and $\text{Cos}(q) \triangleq [\cos(q_1), \cos(q_2), \cos(q_3)]^T$. Besides, the inertial force contribution at the rear arm level can be formulated as follows:

$$\Gamma_{arm} = I_{arm}\ddot{q} \quad (20)$$

where $I_{arm} \in \mathbb{R}^{3 \times 3}$ is a diagonal inertia matrix including the inertia of actuators, rear arms, and half-masses of the forearms.

Regarding the traveling-plate forces G_{tp} and F_{tp} , they are mapped from actuators side to torque contributions using the Jacobian matrix as follows:

$$\Gamma_{G_{tp}} = J^T G_{tp} \quad (21)$$

$$\Gamma_{F_{tp}} = J^T F_{tp} \quad (22)$$

After applying the virtual work principle, and using the differential kinematic model, one can establish the inverse dynamic model of Delta PKM as follows:

$$\Gamma = M(q)\ddot{q} + C(q, \dot{q})\dot{q} + G(q) \quad (23)$$

where $M(q) = I_{arm} + J^T M_{tp} J$ is the total mass and inertia matrix, $C(q, \dot{q}) = J^T M_{tp} \dot{J}$ is the Coriolis and centrifugal forces matrix, $G(q) = -\Gamma_{G_{tp}} - \Gamma_{G_{arm}}$ is the gravitational forces vector, and Γ is the control input vector (i.e. torques generated by the actuators). The main dynamic parameters of Delta PKM are summarized in Table I.

TABLE I
THE MAIN DYNAMIC PARAMETERS OF DELTA PKM.

Parameter	Description	Value
L	Rear-arm length	240 mm
l	Forearm length	480 mm
m_r	Rear-arm mass	0.22 kg
m_f	Forearm mass	0.084 kg
m_p	Traveling-plate mass	0.065 kg
I_{act}	Actuator inertia	1.82×10^{-3} kg.m ²

V. REAL-TIME EXPERIMENTS AND RESULTS

In order to validate the relevance of the proposed control solution for the trajectory tracking problem of PKMs, we implemented the following controllers on Delta PKM: the standard ST-SMC, the feedforward ST-SMC, and the proposed adaptive feedforward ST-SMC. A comparative study is conducted among these three controllers through two experimental scenarios, including the (i) nominal case and (ii) robustness towards operating acceleration changes. In this section, we present the experimental implementation conditions, the obtained results, and a discussion.

A. Experimental platform and implementation issues

1) *Experimental setup*: The experimental platform of Delta parallel robot used for validation of the above controllers is illustrated in Fig. 3. This platform is located at the Robotics Systems Laboratory of EPFL in Switzerland. The three rotational actuators driving the robot are direct-drive motors. Each actuator can deliver up to 23 Nm as maximum applied torque. A desktop computer running under Windows XP operating system allows the programming of Delta robot. The control loop operates with a sampling frequency of 1 KHz (i.e. a sample time of 1 ms).

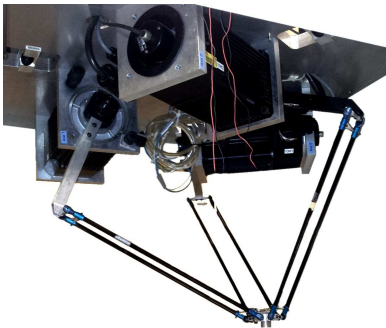


Fig. 3. View of the experimental platform of Delta PKM.

2) *Reference trajectory*: The reference trajectory of the Delta parallel robot is composed of a group of repetitive semi-elliptic geometric motions. It appears in the form of pick-and-place trajectory used usually for various industrial packaging applications. A 3D-view illustrating the reference trajectory in Cartesian space is shown in Fig. 4.

3) *Performance indicators*: Our main objective is to enhance the trajectory tracking performance of parallel manipulators. Then, in order to quantify this performance improvement, the Root-Mean-Square-Error (RMSE) criterion has been adopted. The RMSE in Cartesian space is given as

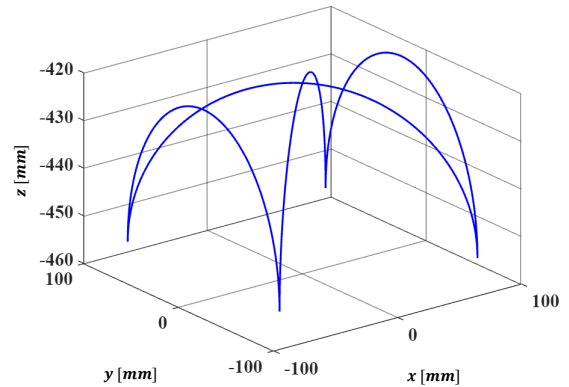


Fig. 4. 3D illustrative view of the pick-and-place reference trajectory.

follows:

$$RMSE_T = \sqrt{\frac{1}{N} \sum_{i=1}^N (e_x^2(i) + e_y^2(i) + e_z^2(i))} \quad (24)$$

where e_x , e_y , e_z represent the position tracking errors along the three translational axes, x , y , and z respectively, and N is the number of registered samples for the whole trajectory. In a similar manner, the RMSE in joint space is expressed as follows:

$$RMSE_J = \sqrt{\frac{1}{N} \sum_{i=1}^N (e_{q_1}^2(i) + e_{q_2}^2(i) + e_{q_3}^2(i))} \quad (25)$$

where e_{q_1} , e_{q_2} , e_{q_3} represent the joint position tracking errors of the three joint angles.

4) *Tuning of the control gains*: The control gains are tuned in real-time experiments based on Trial-and-Error method. This method is usually used when there is no exact matching between the dynamic model and the real system, such that numerical tuning methods fail to give adequate control gains for real-time framework. The resulting feedback gains in real-time experiments are summarized in Table II for the three implemented controllers: standard ST-SMC, feedforward ST-SMC, and adaptive feedforward St-SMC.

TABLE II
THE CONTROL GAINS OF THE THREE CONTROLLERS.

Standard ST-SMC	FF-ST-SMC	Proposed AFF-ST-SMC
$\lambda = 360$	$\lambda = 360$	$\lambda = 360$
$K_2 = 0.05$	$K_1 = 0.25$	$K_1 = 0.25$
$K_3 = 1.5$	$K_2 = 1.5$	$K_2 = 1.5$
	$K_3 = 2$	$K_3 = 2$
		$\Xi = 0.1$

B. Obtained results

For pick-and-place motions, the moving platform's mass is subject to time variations. Consequently, in order to assess our proposed adaptive feedforward ST-SMC controller, we propose to estimate the moving platform's mass in both adopted scenarios. It is worth to note that the estimated parameter \hat{m}_{tp} includes the mass of the traveling-plate and half-masses of the forearms.

1) *Scenario 1 - nominal case:* In this scenario, the parallel robot is controlled to operate at an acceleration of 2.5 G following the reference trajectory illustrated in Fig. 4.

The evolution of Cartesian tracking errors of the three implemented controllers is depicted in Fig. 5. For a purpose of clarity, a zoomed-in view of the Cartesian tracking errors within the interval [5.5, 6.5] sec is depicted in Fig. 6. The obtained results show that the proposed controller outperforms both the standard and feedforward ST-SMC algorithms in terms of tracking performance. The evaluation of the three controllers is summarized in Table. III. Significant improvements (up to 83 %) can be noticed for the proposed controller with respect to the standard ST-SMC in terms of both Cartesian and joint tracking errors. Moreover, good improvements (up to 13.6 %) are also achieved by the proposed controller with respect to the feedforward ST-SMC in terms of both Cartesian and joint tracking errors.

Starting from zero, the moving platform's mass estimation converges to its steady-state value within 5 sec as shown in Fig. 7. Thereafter, it continues adapting to the variation of system states leading to a better control performance.

The generated input torques by the three controllers are depicted in Fig. 8. It is clear that the three controllers generate input torques within the admissible range of robot actuators. The frequency of generated torques appears enough acceptable to execute the safely trajectory cycles. It is worth to note that the control efforts for the proposed adaptive controller are slightly reduced compared to the non-adaptive controllers.

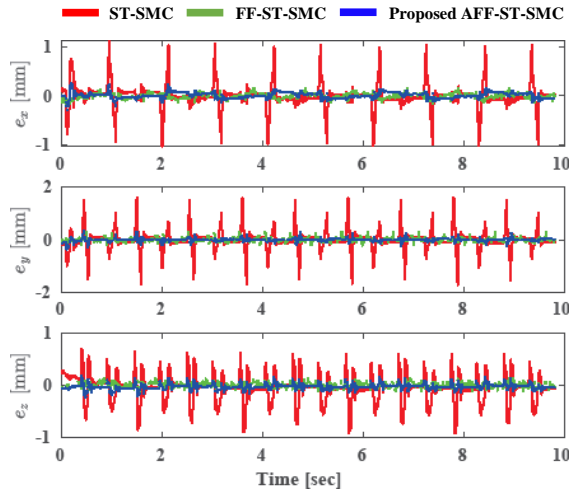


Fig. 5. Scenario 1: Evolution versus time of the Cartesian tracking errors.

TABLE III
SCENARIO 1: PERFORMANCE EVALUATION OF THE THREE CONTROLLERS.

	$RMSE_T$ [mm]	$RMSE_J$ [deg]
Standard ST-SMC	0.5278	0.1297
Feedforward ST-SMC	0.1031	0.025
Proposed AFF-ST-SMC	0.089	0.0216
Improvements w.r.t ST-SMC	83.14 %	83.35 %
Improvements w.r.t FF-ST-SMC	13.68 %	13.6 %

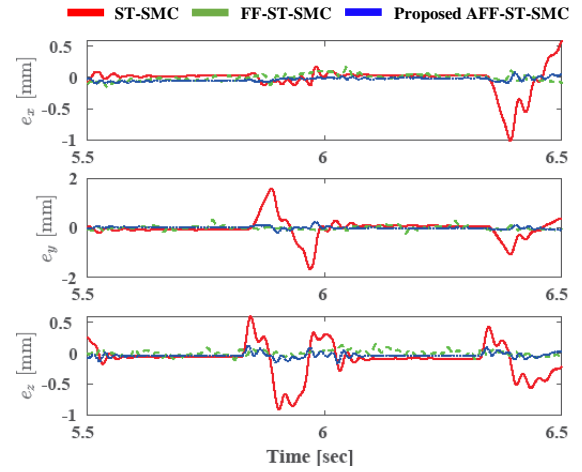


Fig. 6. Scenario 1: Zoomed-in view of the Cartesian tracking errors.

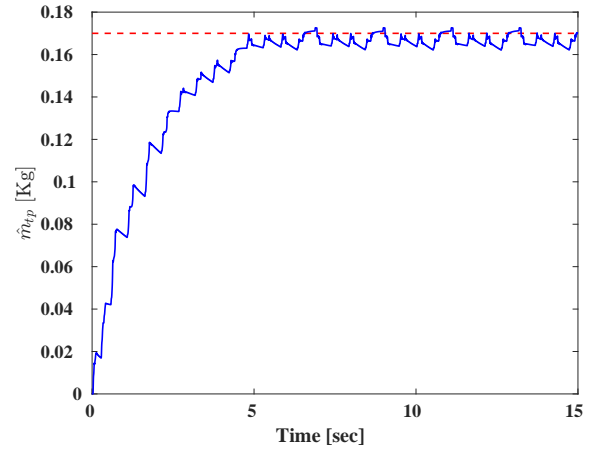


Fig. 7. Scenario 1: Evolution versus time of the estimated moving platform's mass.

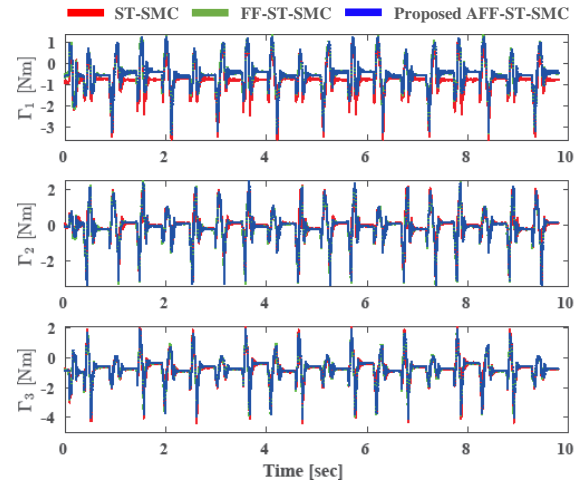


Fig. 8. Scenario 1: Evolution versus time of the control input torques.

2) *Scenario 2: robustness towards operating acceleration changes:* In this scenario, the operating acceleration is increased up to 10 G. Considering the scenario of high-speed accelerations is important to evaluate the performance of the

proposed controller for pick-and-place applications.

The evolution of Cartesian tracking errors of the three implemented controllers is plotted in Fig. 9. A zoomed-in view of the Cartesian tracking errors within the interval [5.5, 6.5] sec is depicted in Fig. 10. The results confirm once again that the proposed controller outperforms both the standard and feedforward ST-SMC algorithms in terms of tracking performance, even with the change of dynamic operating conditions (increase of acceleration). The performance evaluation of the three controllers is summarized in Table. IV. Significant improvements are achieved by the proposed controller with respect to the standard ST-SMC in terms of Cartesian and joint tracking errors, with up to 76 % and 75 % respectively. Moreover, good improvements are also achieved by the proposed controller with respect to the feedforward ST-SMC in both Cartesian and joint spaces.

The moving platform's mass estimation converges to its steady-state value within less than 2 sec as shown in Fig. 11. Thereafter, it continues adapting to the variation of system states resulting in an improved control performance. It is worth to note that the converging time of the estimated parameter to its steady-state value is reduced compared to scenario 1. This can be explained by an inverse proportional relationship between the time constant of the differential equation solution of the adaptation law dynamics and the dynamic errors. By the increase of dynamic errors at high-speed operating conditions, the time constant decreases and the rate of change of the estimated parameter increases, thanks to the adaptation law.

The control input torques generated by the three controllers are displayed in Fig. 12. Similarly to scenario 1, the three controllers generate input torques within the admissible range of the robot actuators, no high-frequency components appear, and the control efforts of the proposed adaptive controller are less than those of non-adaptive ones.

C. Discussion

A comparative study among the three implemented controllers, including the standard ST-SMC, the feedforward ST-SMC, and the proposed adaptive feedforward ST-SMC is conducted. The obtained experimental results have shown the superiority of the model-based controllers compared to the non-model-based controller. Moreover, considering a dynamic parameter adaptation within the closed-loop control improves the dynamic performance of the parallel manipulator in terms of accuracy. This can be referred to the fact that adaptation can estimate more precisely the dynamic model that satisfies operating condition changes while executing a certain task. Relying on the desired trajectories to compute the dynamic model provides the control algorithm robustness towards measurements noise, and, correspondingly, leads to a better global performance. Thanks to the designed adaptation law, the parameter estimation preserves stability overall the reference trajectory. Moreover, it ensures a better convergence time to the steady-state parameter value as operating acceleration increases, which can be relevant for high-speed pick-and-place applications.

VI. CONCLUSION AND FUTURE WORK

In this work, a novel adaptive feedforward super-twisting sliding mode control algorithm for tracking control problem of PKMs has been proposed. Real-time experimental tests have been conducted on a Delta parallel robot showing better performances of the proposed controller, compared to the standard and the feedforward super-twisting algorithms in

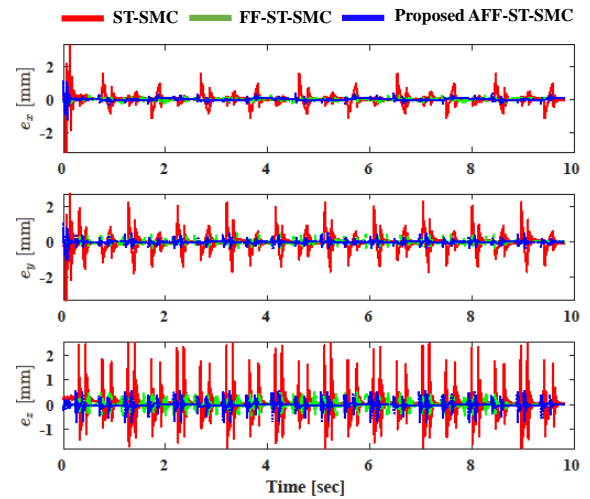


Fig. 9. Scenario 2: Evolution versus time of the Cartesian tracking errors.

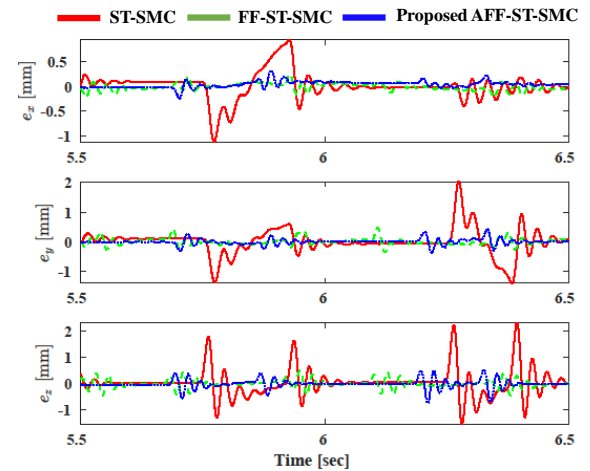


Fig. 10. Scenario 2: Zoomed-in view of the Cartesian tracking errors.

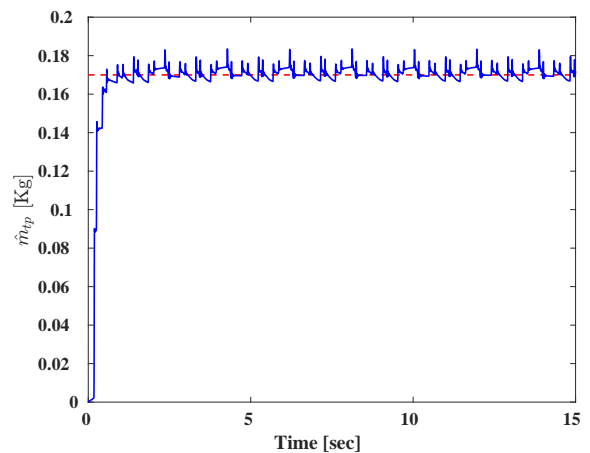


Fig. 11. Scenario 2: Evolution versus time of the estimated moving platform's mass.

terms of tracking precision and robustness towards operating acceleration changes. For future works, one can address the theoretical stability analysis of the proposed controller.

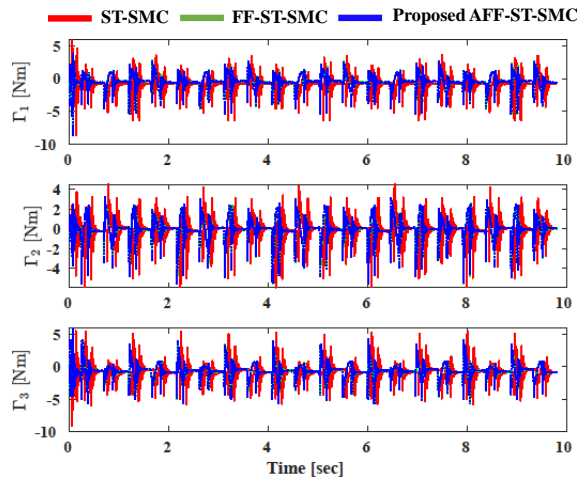


Fig. 12. Scenario 2: Evolution versus time of the control input torques.

Moreover, the adaptation law can be updated to estimate more dynamic parameters such as inertial effects, etc.

REFERENCES

[1] C. Connolly, "ABB high-speed picking robots establish themselves in food packaging," *Industrial Robot: An International Journal*, vol. 34, no. 4, pp. 281–284, Jan. 2007.

[2] J. M. Escorcia-Hernandez, A. Chemori, H. Aguilar-Sierra, and J. A. Monroy-Anieva, "A new solution for machining with r-pkms: Modelling, control and experiments," *Mechanism and Machine Theory*, vol. 150, p. 103864, 2020, doi: 10.1016/j.mechmachtheory.2020.103864.

[3] M. Wapler, V. Urban, T. Weisener, J. Stallkamp, M. Dürr, and A. Hiller, "A Stewart platform for precision surgery," *Transactions of the Institute of Measurement and Control*, vol. 25, no. 4, pp. 329–334, Oct. 2003.

[4] G. Hassan, M. Gouttefarde, A. Chemori, P.-E. Hervé, M. E. Rafei, C. Francis, and D. Sallé, "Time-Optimal Pick-and-Throw S-Curve Trajectories for Fast Parallel Robots," *IEEE/ASME Transactions on Mechatronics*, pp. 1–11, 2022.

[5] U. Asif, "Design of a Parallel Robot with a Large Workspace for the Functional Evaluation of Aircraft Dynamics beyond the Nominal Flight Envelope," *International Journal of Advanced Robotic Systems*, vol. 9, no. 2, p. 51, Aug. 2012.

[6] J. G. Ziegler and N. B. Nichols, "Optimum Settings for Automatic Controllers," *Journal of Dynamic Systems, Measurement, and Control*, vol. 115, no. 2B, pp. 220–222, June 1993.

[7] B. Duan, Y. Su, and C. Zheng, "Nonlinear PID control of a six-DOF parallel manipulator," *IEE Proceedings - Control Theory and Applications*, vol. 151, no. 1, pp. 95–102, Jan. 2004.

[8] H. Saied, A. Chemori, M. Bouri, M. El Rafei, C. Francis, and F. Pierrot, "A new time-varying feedback RISE control for second-order nonlinear MIMO systems: theory and experiments," *International Journal of Control*, vol. 94, no. 8, Aug. 2021.

[9] R. Kumar, A. Chalanga, and B. Bandyopadhyay, "Smooth integral sliding mode controller for the position control of Stewart platform," *ISA Transactions*, vol. 58, pp. 543–551, Sept. 2015.

TABLE IV

SCENARIO 2: PERFORMANCE EVALUATION OF THE THREE CONTROLLERS.

	$RMSE_T$ [mm]	$RMSE_J$ [deg]
Standard ST-SMC	0.8205	0.2136
Feedforward ST-SMC	0.2053	0.0545
Proposed AFF-ST-SMC	0.193	0.0514
Improvements/ST-SMC	76.48 %	75.94 %
Improvements/FF-ST-SMC	6 %	5.69 %

[10] C. Yang, Q. Huang, H. Jiang, O. Ogbo Peter, and J. Han, "PD control with gravity compensation for hydraulic 6-DOF parallel manipulator," *Mechanism and Machine Theory*, vol. 45, no. 4, pp. 666–677, Apr. 2010.

[11] Y.-X. Zhang, "Modeling, identification and control of a redundant planar 2-dof parallel manipulator," 2007.

[12] M. Asgari and M. A. Ardestani, "Dynamics and improved computed torque control of a novel medical parallel manipulator: applied to chest compressions to assist in cardiopulmonary resuscitation," *Journal of Mechanics in Medicine and Biology*, vol. 15, no. 04, p. 1550051, Aug. 2015, publisher: World Scientific Publishing Co.

[13] G. Sartori-Natal, A. Chemori, and F. Pierrot, "Dual-space adaptive control of redundantly actuated parallel manipulators for extremely fast operations with load changes," in *Proc. IEEE Int. Conf. Robotics Automat.*, St Paul, MN - USA., 2012.

[14] A. Chemori, R. Kouki, and F. Bouani, "A new fast nonlinear model predictive control of parallel manipulators: Design and experiments," *Control Engineering Practice*, vol. 130, p. 105367, 2023.

[15] M. Honegger, A. Codourey, and E. Burdet, "Adaptive control of the Hexaglide, a 6 dof parallel manipulator," in *Proceedings of International Conference on Robotics and Automation*, vol. 1, Apr. 1997, pp. 543–548 vol.1.

[16] G. S. Natal, A. Chemori, and F. Pierrot, "Dual-Space Control of Extremely Fast Parallel Manipulators: Payload Changes and the 100g Experiment," *IEEE Transactions on Control Systems Technology*, vol. 23, no. 4, pp. 1520–1535, July 2015.

[17] J. M. Escorcia-Hernandez, A. Chemori, and H. Aguilar-Sierra, "Adaptive rise feedback control for robotized machining with pkms: Design and real-time experiments," *IEEE Transactions on Control Systems Technology*, vol. 23, no. 4, pp. 1520–1535, 2022.

[18] M. Bennehar, G. El-Ghazaly, A. Chemori, and F. Pierrot, "A novel adaptive terminal sliding mode control for parallel manipulators: Design and real-time experiments," in *2017 IEEE International Conference on Robotics and Automation (ICRA)*, May 2017, pp. 6086–6092.

[19] A. Levant, "Sliding order and sliding accuracy in sliding mode control," *International Journal of Control*, vol. 58, no. 6, Dec. 1993.

[20] H. Saied, A. Chemori, M. Bouri, M. E. Rafei, and C. Francis, "Feedforward super-twisting sliding mode control for robotic manipulators: Application to pkms," *IEEE Transactions on Robotics*, pp. 1–18, 2023.

[21] S.-H. Chen and L.-C. Fu, "Adaptive super-twisting sliding mode control on hydraulic actuator of a 6-DOF parallel manipulator," in *2015 10th Asian Control Conference (ASCC)*, May 2015, pp. 1–6.

[22] S. Roy, S. Baldi, and L. M. Fridman, "On adaptive sliding mode control without a priori bounded uncertainty," *Automatica*, vol. 111, p. 108650, 2020-01-01.

[23] B. Siciliano and O. Khatib, *Springer handbook of robotics*. Switzerland: Springer, Cham, 2016.

[24] J. A. Moreno and M. Osorio, "A Lyapunov approach to second-order sliding mode controllers and observers," in *2008 47th IEEE Conference on Decision and Control*. Cancun, Mexico: IEEE, 2008, pp. 2856–2861.

[25] C.-S. Jeong, J.-S. Kim, and S.-I. Han, "Tracking Error Constrained Super-twisting Sliding Mode Control for Robotic Systems," *International Journal of Control, Automation and Systems*, vol. 16, no. 2, pp. 804–814, Apr. 2018.

[26] L. Derafa, A. Benallegue, and L. Fridman, "Super twisting control algorithm for the attitude tracking of a four rotors UAV," *Journal of the Franklin Institute*, vol. 349, no. 2, pp. 685–699, Mar. 2012.

[27] S. Mobayen, F. Tchier, and L. Ragoub, "Design of an adaptive tracker for n-link rigid robotic manipulators based on super-twisting global nonlinear sliding mode control," *International Journal of Systems Science*, vol. 48, no. 9, pp. 1990–2002, July 2017.

[28] W. Khalil and E. Dombre, *Modeling, Identification and Control of Robots*, ser. Kogan Page Science paper edition Modeling, identification & control of robots. Elsevier Science, 2004.

[29] R. Clavel, "Device for the movement and positioning of an element in space," *United States Patent, Sogeva SA, 4976582A*, Dec 1990.

[30] M. Bennehar, A. Chemori, and F. Pierrot, "A novel rise-based adaptive feedforward controller for redundantly actuated parallel manipulators," in *Proc. IEEE/RSJ Int. Conf. Intel. Robots and Systems.*, Chicago, IL - USA, 2014.

[31] A. Codourey, "Dynamic Modeling of Parallel Robots for Computed-Torque Control Implementation," *The International Journal of Robotics Research*, vol. 17, no. 12, pp. 1325–1336, Dec. 1998.